

Measurements of Cosmic Rays with IceTop/IceCube: Status and Results

ALESSIO TAMBURRO

Bartol Research Institute and Department of Physics and Astronomy,

University of Delaware, Newark, DE 19716, USA

atamburro@icecube.wisc.edu

Abstract

The IceCube Observatory at the South Pole is composed of a cubic kilometer scale neutrino telescope buried beneath the icecap and a square-kilometer surface water Cherenkov tank detector array known as IceTop. The combination of the surface array with the in-ice detector allows the dominantly electromagnetic signal of air showers at the surface and their high-energy muon signal in the ice to be measured in coincidence. This ratio is known to carry information about the nuclear composition of the primary cosmic rays. This paper reviews the recent results from cosmic-ray measurements performed with IceTop/IceCube: energy spectrum, mass composition, anisotropy, search for PeV γ sources, detection of high energy muons to probe the initial stages of the air shower development, and study of transient events using IceTop in scaler mode.

I. INTRODUCTION

For 100 years since their discovery, primary cosmic rays have been measured with different techniques and at different locations on Earth[1]. Particularly interesting are those cosmic particles in the energy range between $3 \cdot 10^{14}$ eV (300 TeV or 0.3 PeV) and 10^{21} eV (1000 EeV), whose origin, composition, and energy spectrum remain not fully understood. Cosmic magnetic fields permeating all space prevent the localization of the sources that produced the charged particles observed at Earth. In addition, the relatively low flux of these primaries (about $1 \text{ m}^{-2} \cdot \text{yr}^{-1}$ at 10^{15} eV) does not allow for direct measurements. Subsequent interactions in the atmosphere result in air showers of secondary particles that are sampled at ground. These secondaries also release Cherenkov and fluorescence light detected with telescopes.

The IceCube Observatory is a three-dimensional cosmic-ray air shower detector (Fig. 1). The surface component, IceTop, is an array of water Cherenkov tanks that samples the shower at the surface. The deep detectors of IceCube (between 1.45 km and 2.45 km below the surface) measure the signal from penetrating muons, which have 500 GeV or greater at production in the atmosphere. Events seen in coincidence by both the surface and the deep detectors (coincident events) offer a unique view of cosmic-ray air showers because they carry information from two different regions of shower development. The surface shower is dominated by low-energy photons, electrons, and muons produced throughout the cascade, while the high-energy muons reflect the early stage of shower development. In addition to coincident events, it is also possible to use IceTop as a stand-alone air shower array and to use the deep detector by itself as a muon detector. Together, the three types of events allow measurement of the energy spectrum, composition, and anisotropy of the primary cosmic rays from about 10 TeV to about 1 EeV.

The main goal of IceCube is to detect and measure high-energy neutrinos of extra-terrestrial origin, as described in the companion review article in this journal[2]. The high-energy neutrinos are expected to point back to the cosmic-ray sources in which they are produced[3]. From the point of view of neutrino astronomy, IceTop serves as a partial *veto* against atmospheric background in the deep detector.

The emphasis of this paper is to review the apparatus and its performances, and the recent physics results of IceCube as a cosmic-ray detector. The performances will be reviewed in Sec. 2. Current results from cosmic-ray mass composition and energy spectrum analysis will

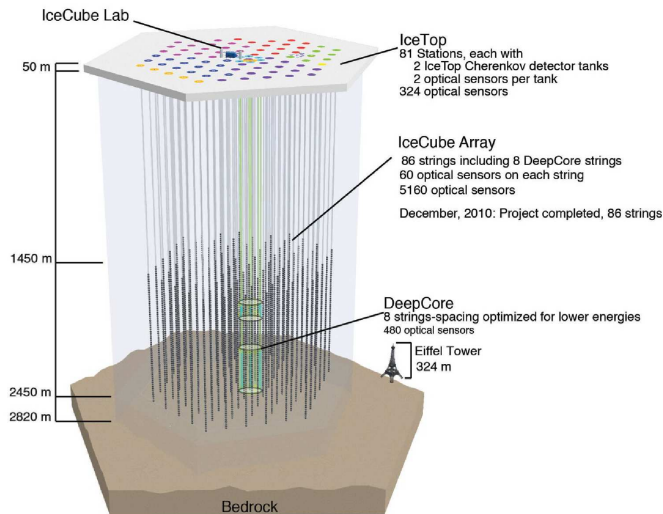


Figure 1: Sketch of the IceCube Observatory labeled with some of its main features. The different colors at the surface identify different deployment stages of the detector. IceCube in its 2006-07 configuration is shown in red and termed as IT26/IC22 (26 IceTop stations/22 in-ice strings). Other configurations are IT40/IC40 (2007-08) in green, IT59/IC59 (2008-09) in violet, IT73/IC79 (2009-10) in blue, and IT81/IC86 (2010-11) in yellow.

be discussed in Sec. 3. The anisotropy measured with IceTop data is presented in Sec. 4. Finally, this paper will also report on recent results including PeV γ search (Sec. 5), high momentum in-ice laterally separated muons (Sec. 6), and detection of transient events (solar flares and gamma-ray bursts) with IceTop (Sec. 7).

II. COSMIC-RAY DETECTION AND RECONSTRUCTION

The IceTop detector[4] is a surface array of 162 cylindrical Cherenkov tanks installed at the 2835 m altitude of the South Pole surface (atmospheric depth of about 680 g/cm^2). The tanks are 1.86 m in diameter and 1.10 m in height. Filled with clear ice to a depth of 0.90 m, they operate on the same principle as the water tanks of the Haverah Park experiment[5] and the Pierre Auger Observatory[6]. To minimize accumulation of drifting snow, the tanks have their top surface level with the surrounding snow. Nevertheless, a variable and not negligible snow coverage is measured and accounted for when analyzing data.

Pairs of tanks, 10 m apart from each other, localize 81 stations that are distributed over an area of about 1 km^2 on a triangular grid with mean spacing of approximately 125 m. An *in-fill* array for denser shower sampling is configured in the center of IceTop by using 3 stations at smaller distances together with their 5 neighboring stations. Each IceTop tank contains two standard IceCube digital optical modules[7, 8] (DOMs), which include light sensor and read-out electronics. To enhance the dynamic range, the DOMs of each tank are run at 2 different gains (low and high) with resulting effective thresholds of 20 and 200 photoelectrons (pe), respectively. Cosmic-ray muons, hitting the tanks at an approximate rate of 2 kHz, provide the basic calibration of tanks. The signal spectrum of a tank consists of a low-energy electromagnetic component and a muon peak at higher energy. The tank signals are calibrated in units of “vertical equivalent muon” or VEM whose definition is based on the muon peak of the tank spectrum. A vertically through-going muon of about 1 GeV produces approximately 125 pe in

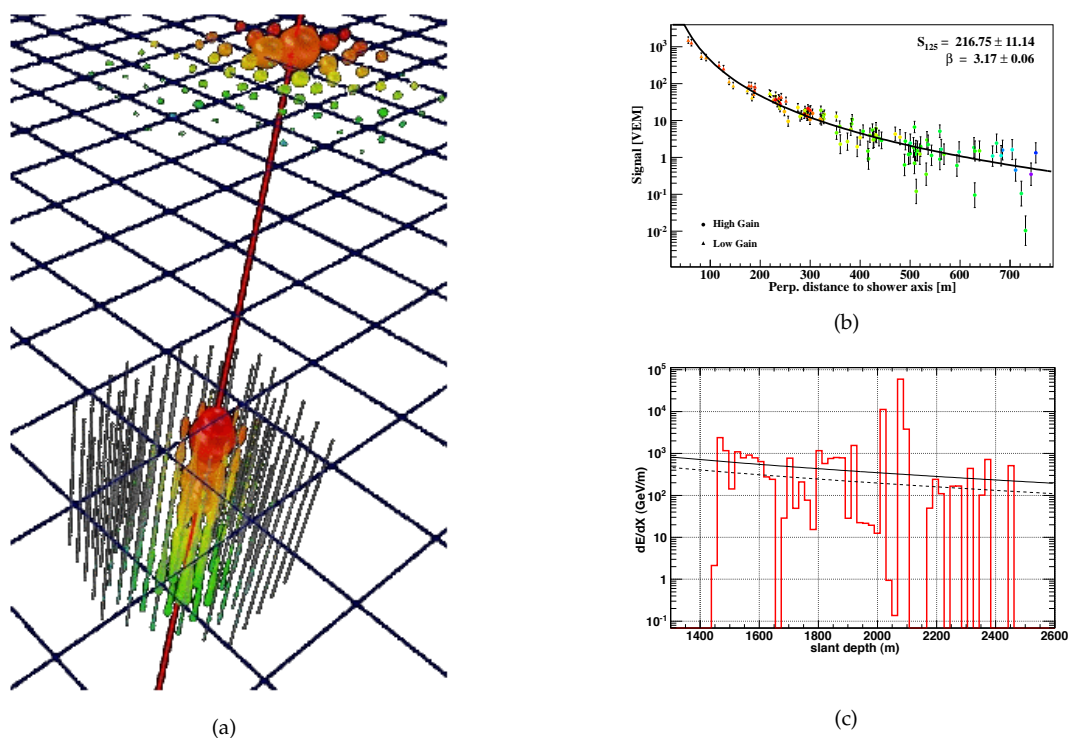


Figure 2: (a) Coincident event recorded by IceTop/IceCube in 2010 (IT73/IC79). The triggered DOMs are indicated with colored spheres with radii proportional to the signal. (b) Lateral distribution of tank signals in VEM for the event in Fig. 2(a) fitted to a double logarithmic parabola (see text for details). (c) Muon energy loss dE/dX as a function of the in-ice depth for the event in Fig. 2(a). The stochastic energy loss is about 880 GeV/m above the fitted average energy loss (black line). The dashed line is the average energy loss after removal of the stochastic peaks.

a high-gain DOM. In addition to measuring signal amplitudes, the IceTop DOMs can record the counting rate of low-energy cosmic rays (scaler mode). The rates are available for heliospheric studies of solar modulation and transient events such as solar flares and gamma-ray bursts (GRBs).

To initiate the readout of a DOM, its neighbor in the other tank at the same station has to be hit (hard local coincidence or HLC). This suppresses the background of accidental signals caused by isolated muons and allows a good angular resolution. The basic IceTop air shower trigger requires 6 DOMs to “launch” or report signals within a $5 \mu\text{s}$ time window. Thus, even if only high-gain DOMs are above threshold, this trigger includes all 3-station events. The rate for these events is 30 Hz. Once the trigger is formed, additional signals from single tanks are added if they occur within a $20 \mu\text{s}$ time window (soft local coincidence or SLC). Counting SLCs is useful to evaluate the shower muon content. These SLC signals are also read out when an in-ice trigger forms either with or without the presence of HLC signals. In this case, SLCs can be used to veto down-going cosmic rays when measuring up-going neutrinos.

There are different topologies of events that are relevant for analysis of cosmic-ray data with IceTop/IceCube. This paper will concentrate on results obtained with analysis of events caused by nearly vertical (zenith angles $\theta \lesssim 37^\circ$ or $\cos\theta > 0.8$) and contained air showers (Fig. 2(a)). These showers are reconstructed with their axis crossing both parts of the detector. The effective area of IceCube for such coincident events is $A \approx 0.15 \text{ km}^2\text{sr}$. The maximum energy above which the intensity is too low to obtain enough events for analysis is about 1 EeV. The effective area rises to $0.4 \text{ km}^2\text{sr}$ for detecting events by IceTop alone.

The surface shower particle density decreases rapidly with the distance from the shower axis (lateral distribution function). This lateral distribution carries information about the energy of the primary particles. The charge expectation value S in an IceTop tank at distance r from the shower axis is described with a “double logarithmic parabola” (Fig. 2(b)) as follows[9]

$$S(r) = S_{ref} \cdot \left(\frac{r}{R_{ref}} \right)^{-\beta - \kappa \log_{10}(r/R_{ref})}, \quad (1)$$

where $R_{ref} = 125$ m, S_{ref} is the charge in VEM at R_{ref} , and $\kappa = 0.303$. The parameter S_{ref} is thus referred to as S_{125} and is a measurement of the shower size. The signals measured between about 30 m and 300 m from the shower axis are quite well described by Eq. 1 for primary energies in the range 1–100 PeV and arrival directions with zenith in the range 0° – 40° .

The arrival time behind the shower plane, $\Delta t(r)$, as a function of the lateral distance r from the shower axis is described by the sum of a parabola and a Gaussian function, both symmetric around the shower axis, with the following form

$$\Delta t(r) = ar^2 + b \left(\exp \left(\frac{r^2}{2\sigma_r^2} \right) - 1 \right), \quad (2)$$

where $a = 4.823 \cdot 10^{-4}$ ns/m², $b = 19.41$ ns, and $\sigma_r = 83.5$ m. The energy, zenith angle, and mass dependence of a , b , and σ_r is currently under investigation in simulations. When reconstructing the shower direction \vec{n} , Eq. 2 accounts for the shower front curvature as follows

$$t(\vec{x}) = t_0 + \frac{\vec{x} - \vec{x}_c}{c} \vec{n} + \Delta t(r), \quad (3)$$

where $t(\vec{x})$ is the tank signal time, \vec{x} the tank position, \vec{x}_c the shower core position, and t_0 the time when the core reaches the surface. For events triggering 5 or more stations, Eq. 3 is fitted to the measured signal times with 5 free parameters, 3 for core position and time, and 2 for shower direction. At the same time, Eq. 1 is fitted to the measured tank signals with 2 free parameters, S_{125} and β . A maximum likelihood method is adopted to obtain the best fit to the measurements[4]. For events triggering 3 or 4 stations, only S_{125} and β are kept free after fitting the measured signal times to obtain core position and time, and shower direction.

The position of IceTop at the high altitude of the South Pole makes it possible to sample ground particles near the shower maximum, thus reducing significantly the effects of fluctuations and allowing accurate measurements. Events of 5 or more stations are expected from primaries of energy between PeV and EeV, whereas 3 or 4 station events set the threshold for cosmic ray detection with IceTop to about 300 TeV. Lower energies ($\gtrsim 100$ TeV) are expected if the events triggering the denser in-fill array are considered. The energy resolution is estimated to be $\lesssim 0.1$ in units of $\log_{10}(E/\text{GeV})$ above about 1 PeV, reaching about 0.05 for $E > 10$ PeV. The angular resolution ranges from about 1° at 10^{15} eV to about 0.2° at 10^{17} eV. The core resolution ranges from about 15.0 m at 10^{15} eV to about 6 m at 10^{17} eV.

Analysis of IceCube coincident events aims to give clear insights into the nuclear composition of cosmic rays for energies that span from PeV to EeV. For a given primary energy, penetrating muons are more abundant in iron showers than in proton showers since their development starts higher in the atmosphere. The muon bundle size is therefore larger for iron showers. On the other hand, proton showers reach their maximum development deeper in the atmosphere than iron showers and the ratio of muons to electrons and photons is therefore smaller at the surface. The number of in-ice muons or muon multiplicity is closely related to the amount of energy deposited in the detector, which is proportional to the amount of Cherenkov light generated. For example, depending on the mass of the primary particle (proton or iron), an event of $5 \cdot 10^{15}$ eV is expected to carry 30 to 80 muons with sufficient energy

to reach a depth of 1500 m and deposit $5 \cdot 10^{12}$ eV to $15 \cdot 10^{12}$ eV in the deep detector. Analogous to surface measurements of tank signals, the in-ice DOM signals (in photoelectrons) can be described in terms of a lateral distribution, which is a function of the distance from the muon bundle track at a given slant depth from the surface. This function is dominated by a decaying exponential whose slope is the attenuation length of light in the ice[10]. The bundle size, termed as K_{70} , is defined as the in-ice signal measured at a slant depth of 1950 m and at a perpendicular distance from the track of 70 m. This observable has been used in combination with S_{125} to discriminate between light and heavy primary masses (see Sec. 3). A different approach explored the reconstruction of the muon bundle energy loss dE/dx to find composition sensitive properties of bundles[11]. The muon bundle energy loss as a function of the slant depth is a convolution of the shower muon multiplicity, the muon energy distribution and the energy loss of a single muon. For iron showers, the bundle energy loss is expected to be greater. Furthermore, for the same amount of energy deposited, stochastic losses along the bundle track are larger in proton showers, which produce more high energy muons.

The reconstruction of air showers with IceTop/IceCube is affected by several uncertainties. These uncertainties have been extensively investigated and several advances are expected in the future results. Pressure variations at the surface and snow coverage affect the measurement of S_{125} with the latter giving the largest contribution. For a given primary energy and arrival direction, higher pressure makes the primary interaction depth shallower thus reducing the shower size. The snow over each tank is physically measured every year and also estimated from the muon/electron ratio in calibration curves. The snow mainly affects the response of the tank to the electromagnetic component of the shower front thus affecting the energy threshold. The shower size is corrected for pressure and snow coverage. Other systematic uncertainties affect the in-ice reconstruction: the ice model used to describe the properties of the photon propagation[12] ($\pm 10\%$), the DOM efficiency[13] ($\pm 10\%$), and the muon rate seasonal variation[14].

III. COSMIC-RAY ENERGY SPECTRUM AND NUCLEAR COMPOSITION

Most galactic cosmic rays are believed to be accelerated in the blast waves (diffusive shocks) of nearby supernova remnants[15] (SNRs) and in some cases (extended sources/strong magnetic fields) can escape the acceleration region with energies up to about 10^{18} eV. The signature of these sources is the gradual steepening of the cosmic-ray flux at a few 10^{15} eV, called *knee*. The well-known power-law form of the cosmic-ray energy spectrum $dN/dE \propto E^{-2.7}$ changes its spectral index to about -3.0. The knee is interpreted as the maximum energy reached through acceleration in SNRs. This energy scales with the charge of the nucleus. Therefore, the spectrum of galactic cosmic rays is predicted to end at energies of about 10^{18} eV with the heaviest elements being accelerated[16]. Depending on whether the transition is from galactic iron to extragalactic proton or from galactic iron to extra-galactic mixed composition of different nuclei, the transition energy is predicted[17] at few 10^{17} eV or few 10^{18} eV. At energies between 10^{15} eV to 10^{17} eV, all air shower experiments observe energy dependent changes of composition that are compatible with an increase of the measured average mass of cosmic rays. Above 10^{17} eV and up to 10^{18} eV measurements of composition indicate a decrease of the cosmic-ray average mass[18]. The cosmic-ray flux up to 10^{17} eV is believed to be mostly dominated by the contribution of galactic sources. The “fingerprint” of the transition to the extra-galactic contribution is expected in the measurement of the mass composition at this energy and above. At the highest energies (above 10^{19} eV), measurements from the Pierre Auger Observatory, and HiRes/Telescope Array give opposite results[19, 20, 21]. These experiments are extending their detectors to reach about 10^{18} eV and below[22, 23, 24], and their measurements will overlap with IceCube measurements.

IceCube/IceTop allows for precise measurements of the primary energy spectrum in a wide

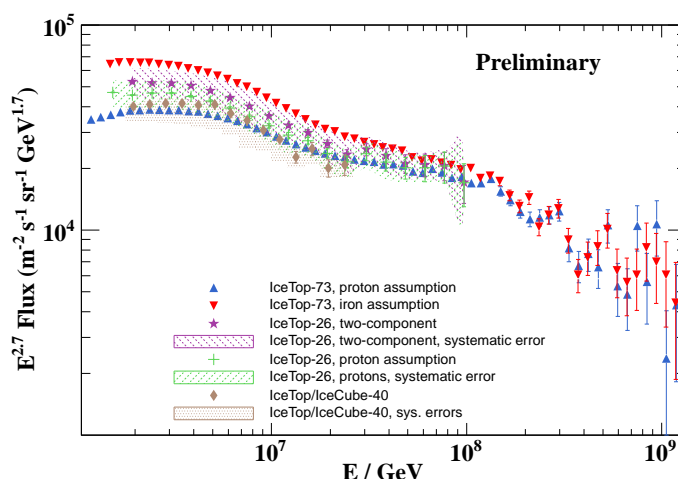


Figure 3: Energy spectra obtained with data of IceTop running in different configurations (IT26, IT40, and IT73). For the IT26 and IT40 spectrum, the systematic uncertainty is also shown.

energy range that reaches the energy threshold of the largest air shower arrays and is sensitive to cosmic-ray nuclear composition changes. The first analysis to determine the all-particle energy spectrum with IceTop[25] was based on data of IT26 (area of 0.094 km²) taken between June and October 2007. In this analysis, the measured shower size (S_{125}) spectra in three zenith angle ranges up to 46° are unfolded or de-convoluted into the estimated energy spectrum. The spectrum obtained in the energy range between 1 and 100 PeV is shown in Fig. 3 along with other spectra measured with IceTop data and discussed in this section. The energy at which the lines with the minimum and maximum slope before and after the knee intersect identifies the knee position. Assuming pure iron, the energy spectra measured in different zenith angle ranges have been shown to disagree and prove that pure iron primaries can be excluded in the energy range up to 25 PeV. A consistent interpretation of the spectra measured at different zenith angles requires a mixed composition. For a two-component model, the knee measured in the IT26 spectrum is at 4.32 PeV and the spectral index above the knee is -3.11. An indication of a flattening of the spectrum above 22 PeV is also observed with a spectral index changing to -2.85.

A preliminary measurement of the spectrum with IT73 has been obtained by analyzing 11 months of data (June 15 to May 13, 2010)[26, 27, 28] (Fig. 3). The statistics is nearly 40,000,000 events between about 0.3 PeV and 1 EeV and for $\cos\theta > 0.8$. Of these events, about 200 are found above about 200 PeV. With enhanced precision, better energy resolution, and larger statistics above 100 PeV, this measurement confirms the earlier result of a flattening observed with IT26 data and reveals the spectrum structure in the steepening between the knee and ankle above about 100 PeV. It also appears that the spectrum is not well described by a single power law. All showers with 5 or more stations and with $\cos\theta > 0.8$ are considered in this analysis. The energy spectrum, now measured between 1 PeV and 1 EeV, will be extended to lower energies, down to 300 TeV. This can be achieved by selecting small events in IceTop[29] and is particularly interesting in view of the recent measurements with ATIC[30] and CREAM[31] balloon-borne calorimeters that are providing increased statistics and a new view of the region around 100 TeV/nucleus.

In Fig. 4, the IceTop spectrum is compared to the spectra obtained with recent measurements of KASCADE-Grande (Karlsruhe, Germany, 110 m a.s.l.)[34, 35], Tibet Array (at Tibet Yangbajing, 4300 m a.s.l.)[36, 37], GAMMA (on the south side of Mount Aragats in Armenia, 3200 m a.s.l.)[38], and Tunka (in the Tunka Valley in Buryatia, Siberia, 675 m a.s.l.)[39]. A

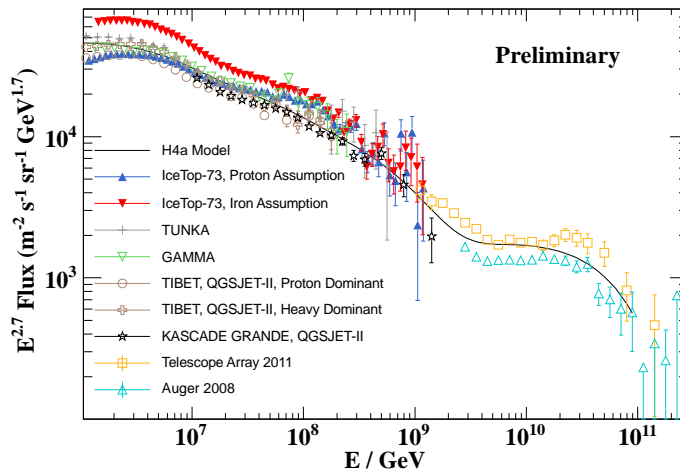


Figure 4: Cosmic-ray energy spectrum measured with IT73 and other experiments operating in the same energy range. The spectra from the Pierre Auger Observatory[32] and Telescope Array[33] are also shown. Finally, the H4a model of the cosmic-ray flux is overlaid (see text for detail).

model assuming three populations of cosmic rays[40] (SNR component, high energy galactic component, and extra-galactic component) and termed as *H4a* is also shown.

A first attempt to measure the mass composition of cosmic rays was performed with one month of data (constant snow coverage) of IceCube in its 2008 IT40/IC40 configuration[10]. A neural network was trained with Monte Carlo simulations of 5 primaries (proton, helium, oxygen, silicon, and iron). Measurements of the electromagnetic component of the air showers at the surface (S_{125}) and the muon component in the ice (K_{70}) are used to “teach” the network how to find the best fit to the primary energy and mass. A measurement of the cosmic-ray energy spectrum (Fig. 3) and composition (Fig. 5) at energies between 1 PeV and 30 PeV was determined. The energy resolution from the neural network ranges from 18–20% in the threshold region of this analysis (1.5 PeV) to 6–8% at 30 PeV, for an average resolution better than 14% over the full range of energies. The energy spectrum derived with this analysis is consistent with other IceTop results within systematic uncertainties. The mean logarithmic mass $\langle \ln A \rangle$ as a function of the primary energy indicates a strong increase in mass through the knee although the systematic uncertainties can greatly affect the measured composition in terms of absolute value of $\langle \ln A \rangle$.

IV. COSMIC-RAY ANISOTROPY MEASUREMENTS

Although detection of γ rays and neutrinos from individual galactic or extra-galactic sources of cosmic rays remains a method to probe the origin of cosmic rays, studies of anisotropy of cosmic-ray arrival directions are important to investigate the characteristics of cosmic-ray propagation in the local interstellar medium.

In IceCube the anisotropy of cosmic-ray arrival directions can be measured in two different ways: using TeV muon events collected with the deep detector or using cosmic-ray air shower events triggering the surface array. The in-ice detector has a lower energy threshold than IceTop, which allows to investigate the anisotropy of cosmic rays at lower primary energies (down to 20 TeV) and larger zenith angles (up to 90°). This makes it possible for the deep detector to reach a higher sensitivity (about $6.3 \cdot 10^{10}$ events/yr, anisotropy level $\delta > 10^{-5}$) and scan small scale structures. On the other hand, IceTop presents a better energy resolution (20% at >300 TeV), although binning is limited by statistics, and potential for including composition

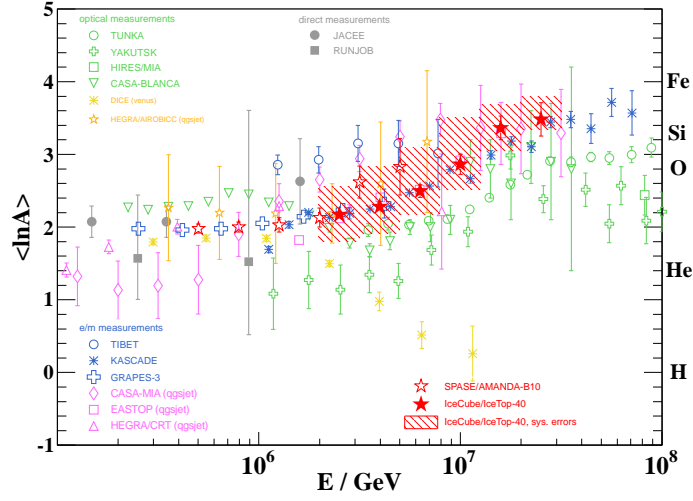


Figure 5: The mean logarithmic mass vs primary energy adapted from Ref. [10]. The IT40/IC40 results are shown with (red) stars along with their statistical errors (solid red error bars) and systematic errors (shaded red region). Measurements from other experiments are also shown. Data points are compiled from Ref. [41, 18].

sensitivity.

A dipole-like large scale anisotropy (amplitude of about 10^{-3}) from few tens of TeV to about 100 TeV has been observed with in-ice data[42, 43]. This anisotropy is inconsistent, both in amplitude and phase, with the Compton-Getting prediction[44], i.e. the apparent anisotropy caused by the relative motion between the Earth and sources of cosmic rays. A small scale anisotropy with significant structure at angular sizes between 10° and 30° has been also observed. This might uncover non-diffusive propagation effects or SNR connection and be a natural consequence of the stochastic nature of cosmic-ray galactic sources, in particular nearby and recent SNRs ($<0.1-1$ kpc)[45, 46, 47].

The analysis of IceTop data confirms and complements the measurement of the large scale anisotropy also at PeV energies[48]. IceTop has an angular resolution of about 3° for energies above 100 TeV and zenith angles up to 40° when pure event geometry reconstruction is performed. The angular resolution degrades to 10° and above for zenith angles greater than 60° . Only events with zenith angles less than 60° are selected ($1.4 \cdot 10^8$ events/yr, $\delta > 10^{-4}$). Monte Carlo studies indicate that the median primary cosmic-ray energy of IceTop data is 640 TeV, with 68% of the events between 200 TeV and 2,400 TeV. Events are classified as low (68% of events in 100–700 TeV, median energy of 400 TeV) and high energy events (68% of events in 0.8–3.8 PeV, median energy of 2 PeV).

Analysis of IceTop data reveals a deficit that confirms what was observed with the in-ice muon analysis at 400 TeV (compare lower left to upper right plot of Fig. 6). The amplitude of this deficit is about $2 \cdot 10^{-3}$ and therefore larger than 10^{-3} observed with in-ice muons. However, these values are in agreement if the uncertainties are considered. Furthermore, above 400 TeV there is indication of an increase in strength of the anisotropy.

V. PEV γ SEARCH

High energy γ rays ($\gtrsim 1$ TeV) have been observed from different galactic sources (SNRs, pulsar wind nebulae, binary systems, the Galactic Center) and extra-galactic sources (starburst galaxies, active galactic nuclei, and objects containing supermassive black holes). At higher

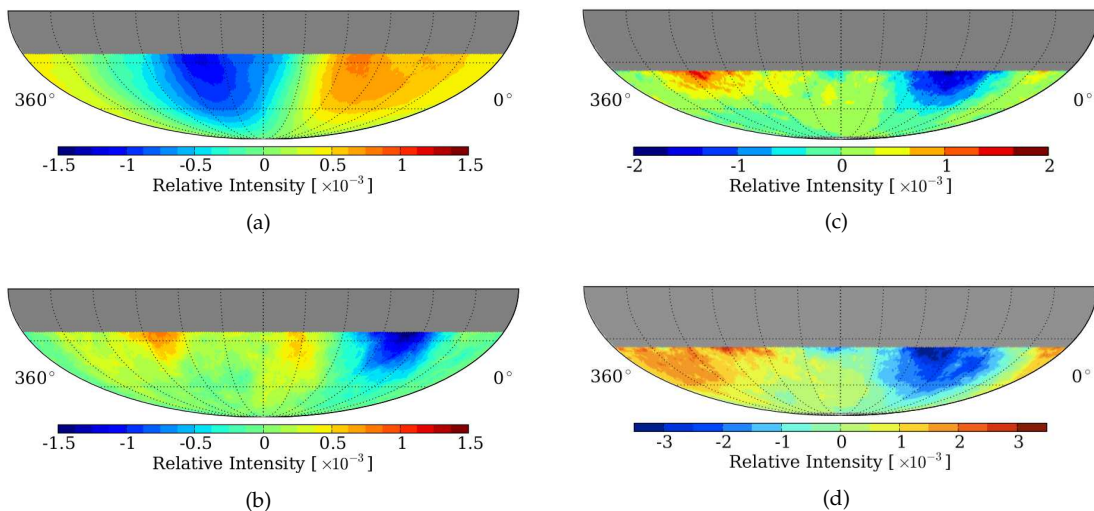


Figure 6: Statistical significance sky maps obtained with IC79 in-ice (left panels) and IT73 IceTop data (right panels). The in-ice data sets have median energies of 20 TeV (upper) and 400 TeV (lower). The IceTop datasets have a median energy of 400 TeV (upper) and 2 PeV (lower). The angular binning or smoothing angle is 20° .

energies ($\gtrsim 100$ TeV), extra-galactic photons are likely to interact with the cosmic microwave background radiation and radiation from infrared starlight from galaxies, producing $e^+ - e^-$ pairs. It is unknown whether galactic sources can emit γ of energy $\gtrsim 100$ TeV. However, a guaranteed diffuse flux of γ rays from interaction of cosmic rays with the interstellar medium and dense molecular clouds is also expected.

IceCube can detect high energy γ rays by *vetoing* on the in-ice component, i.e. searching for showers detected by IceTop where no in-ice activity is observed (muon poor showers)[49]. A PeV γ -ray shower produces about 0.1 muons above 800 GeV. The uncertainties due to the surface detector response and the muon rate production for photon showers are added in quadrature and return an overall systematic uncertainty in sensitivity of 18%. No detectable γ -ray flux has been found by IceCube above 1.2 PeV with one year of data. The fraction of γ in cosmic rays is estimated to be less than $1.2 \cdot 10^{-3}$ (90% *cl*) in the range 1.2–6.0 PeV and within 10° of the galactic plane. IceCube is also sensitive to localized sources, where galactic accelerators or dense targets for extra-galactic cosmic rays might be discovered. It is estimated that at about 1 PeV, IceCube can reveal fluxes as low as about $10^{-19} \text{ cm}^{-2} \text{ s}^{-1} \text{ TeV}^{-1}$ for point sources.

VI. LATERALLY SEPARATED MUONS

High energy muons (>1 TeV) are produced early in air showers and probe the initial shower development. One can distinguish between “conventional” muons, which come from pion and kaon decays, and “prompt” muons, which come from the decays of particles containing heavy quarks, mostly charm. The former are expected to dominate at TeV energies, the latter at higher but uncertain energies. Extending the earlier measurements performed by the MACRO experiment[51], IceCube is capable to resolve muons of cosmic-ray primary interactions and high-energy secondary interactions that are laterally separated by 135 m up to 400 m from the shower core (Fig. 7), where the muon bundle is detected[52]. The separation is due to high transverse momentum of 2–15 GeV/c (corresponding to separations of 135–400 m) transferred to the muon by its parent. Above 2 GeV/c, interactions can be described with perturbative

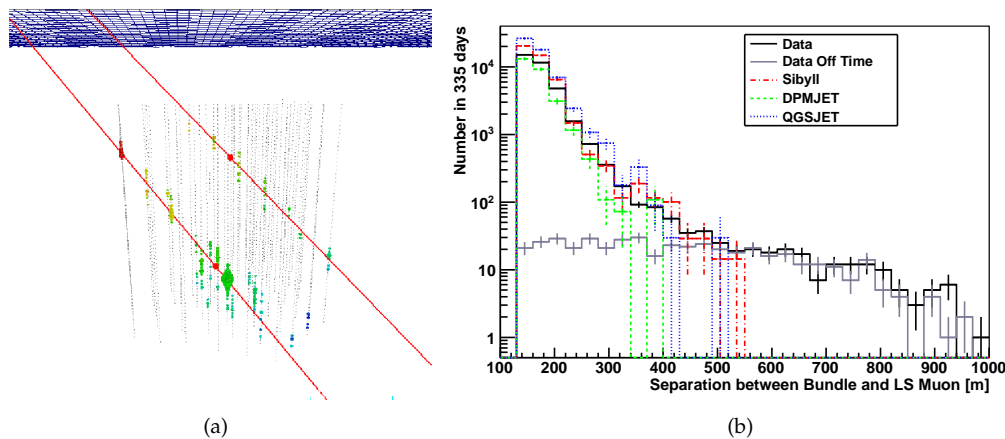


Figure 7: (a) Example of laterally separated muons (upper track) from the muon bundle (lower track) of a cosmic-ray shower reaching the in-ice detector. The separation is 400 m, the angular separation is 3.5° , and the time difference is 20 ns. (b) The separation between the laterally separated (LS) muon and the bundle track after applying all selection criteria for data, simulation with the Sibyll, DPMJET, and QGSJET interaction models, as well as double showers estimated from off-time data.

quantum chromodynamics. However, the cosmic-ray hadronic interaction models used to simulate IceCube events do not reproduce the rates and the zenith angle distributions observed in data.

VII. SOLAR AND HELIOSPHERIC PHYSICS, AND GRB SEARCH

Due to the high altitude and the nearly zero geomagnetic cutoff at the South Pole, secondary particle spectra measured with IceTop retain a significant amount of information on the spectra of the primary particles. IceTop has already demonstrated the novel and unique ability to derive the energy spectrum of solar particles in the multi-GeV regime. The first event detected and studied by IceTop[53] was the solar flare associated to the ground-level event of December 13, 2006. IceTop DOMs can span thresholds from 1 pe to 30 pe corresponding to counting rates of about 8 kHz to about 1 kHz. By taking the differential rates at multiple thresholds, the spectrum of detected events can be studied. Furthermore, IceTop presents 50 times better sensitivity than conventional detectors used for solar and heliospheric physics such as neutron monitors. In addition to solar flares, the typical phenomena studied with IceTop are complex interplanetary disturbances[55] and “Forbush Decreases”[56]. The latter are associated with strong shocks following coronal mass ejections that deplete cosmic rays from the region traversed by the Earth. On May 12, 2012 a significant solar flare was detected by IceTop and is being currently analyzed to determine the energy spectrum (Fig. 8).

An ongoing study shows that IceTop can also reveal GRBs through detection of an overall increase of the counting rates observed in coincidence with the signal recorded on board of dedicated satellites. A flux of γ rays with energies greater than 10 GeV and zenith angles up to about 20° can enhance the counting rate above the steady cosmic-ray background if it is greater than 10^{-5} erg \cdot cm $^{-2}$. IceTop can detect GRBs whose emission extends up to a few 100 GeV and occurring in a sky region not monitored by any other experiment.

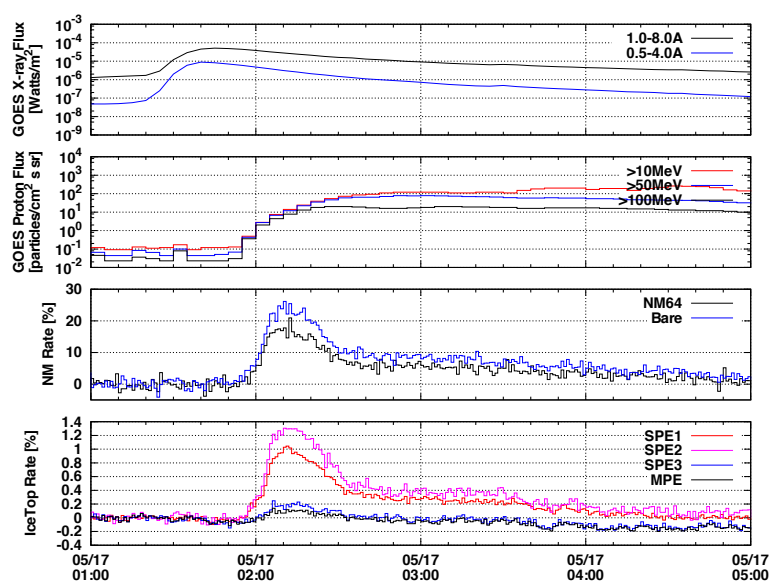


Figure 8: Time profile of the count rate measured by groups of IceTop DOMs with decreasing thresholds (from MPE to SPE3), neutron monitors, and the GOES satellite[54].

VIII. CONCLUSIONS

The IceCube Observatory is currently taking data in the second year after its completion in 2010. Analysis performed with data of the detector in earlier stages of its deployment has been reviewed in this paper. On the one hand, events seen in coincidence by both the surface component, IceTop, and in-ice detectors offer precious information to investigate the mass composition of cosmic rays. On the other hand, analysis of IceTop events allows for precise measurements of the cosmic-ray energy spectrum with large sensitivity. The better understanding of the systematic uncertainties along with the exquisitely large event rate collected will allow IceCube to significantly contribute to shed light on galactic cosmic rays in the near future.

VIII.ACKNOWLEDGMENTS

I am grateful to F. Halzen for the possibility to review IceTop results and to T. Gaisser, H. Kolanoski, and T. Stanev for helpful discussions. A special thanks goes to T. Feusels, L. Gerhardt, T. Kuwabara, B. Ruzybayev, and M. Santander for providing plots. This research is supported in part by the U.S. National Science Foundation Grant NSF-ANT-0856253.

VIII.REFERENCES

- [1] K. H. Kampert and A. A. Watson, *Eur. Phys. J. H* **37**, 3 (2012).
- [2] I. Taboada, *Modern Physics Letters A*. This Series.
- [3] T. K. Gaisser and T. Stanev, *Astropart. Phys.*, In Press, *arXiv* 1202.0310 (2012).
- [4] R. Abbasi *et al.* [IceCube Collaboration], *arXiv* 1207.6326 (2012).
- [5] M. A. Lawrence, R. J. O. Reid, and A. A. Watson, *J. Phys. G* **17**, 733–757 (1991).
- [6] J. Abraham *et al.* [Pierre Auger Collaboration], *Nucl. Instrum. Methods A* **523**, 50–95 (2004).

- [7] R. Abbasi *et al.* [IceCube Collaboration], *Nucl. Instrum. Methods A* **601**, 294 (2009).
- [8] A. Achterberg *et al.* [IceCube Collaboration], *Astropart. Phys.* **26**, 155 (2006).
- [9] S. Klepser, Ph.D. thesis, Humboldt-Universität zu Berlin (2008).
- [10] R. Abbasi *et al.* [IceCube Collaboration], *arXiv* 1207.3455 (2012).
- [11] T. Feusels *et al.* [IceCube Collaboration], in *Proc. of ICRC 2009*, *arXiv* 0912.4668.
- [12] D. Chirkin for the IceCube Collaboration, in *Proc. of ICRC 2011* **3** (HE.2.3), 161-164.
- [13] R. Abbasi *et al.* [IceCube Collaboration], *Nucl. Instrum. Methods A* **618**, 139 (2010).
- [14] S. Tilav *et al.* [IceCube Collaboration], *arXiv* 1001.0776 (2010).
- [15] A. M. Hillas, *J. Phys. G* **31**, R95 (2005).
- [16] P. Blasi and E. Amato, *JCAP* **1201**, 010 (2012). [*arXiv* 1105.4521].
- [17] V. Berezhinsky, in *Proc. of ICRC 2007*, *arXiv* 0710.2750.
- [18] K. H. Kampert and M. Unger, *Astropart. Phys.* **35**, 660 (2012).
- [19] J. Abraham *et al.* [Pierre Auger Collaboration], *Phys. Rev. Lett.* **104**, 091101 (2010).
- [20] R. U. Abbasi *et al.* [HiRes Collaboration], *Phys. Rev. Lett.* **104**, 161101 (2010).
- [21] H. Sagawa [Telescope Array Collaboration], *AIP Conf. Proc.* **1367**, 17 (2011).
- [22] I. C. Maris [Pierre Auger Collaboration], in *Proc. of ICRC 2011* **1** (HE.1), 267-270. [*arXiv* 1107.4809].
- [23] T. H. J. Mathes [Pierre Auger Collaboration], in *Proc. of ICRC 2011* **3** (HE.1.4), 149-152. [*arXiv* 1107.4807].
- [24] S. Ogio [Telescope Array Collaboration], *AIP Conf. Proc.* **1367**, 132 (2011).
- [25] R. Abbasi *et al.* [IceCube Collaboration], *arXiv* 1202.3039 (2012).
- [26] A. Tamburro for the IceCube Collaboration, To appear in *Proc. of 13th Marcel Grossmann Meeting*, Sweden (2012).
- [27] S. Tilav for the IceCube Collaboration, To appear in *Proc. of ISVHECRI 2012*.
- [28] B. Ruzybayev, PhD thesis (in preparation), University of Delaware, USA (2012).
- [29] B. Ruzybayev, S. Hussain, C. Xu, and T. K. Gaisser for the IceCube Collaboration, in *Proc. of ICRC 2009*, *arXiv* 0912.0896.
- [30] A. D. Panov *et al.*, *Bull. Russ. Acad. Sci. Phys.* **73**, 564 (2009).
- [31] Y. S. Yoon *et al.*, *Astrophys. J.* **728**, 122 (2011).
- [32] J. Abraham *et al.* [Pierre Auger Collaboration], *Phys. Rev. Lett.* **101**, 061101 (2008).
- [33] D. Bergmann [Telescope Array Collaboration], UHECR2012, CERN (2012).
- [34] W. D. Apel *et al.* [KASCADE-Grande Collaboration], *Phys. Rev. Lett.* **107**, 171104 (2011). [*arXiv* 1107.5885].
- [35] W. D. Apel *et al.* [KASCADE-Grande Collaboration], *arXiv* 1206.3834 (2012).

- [36] M. Amenomori *et al.* [TIBET III Collaboration], *Astrophys. J.* **678**, 1165 (2008).
- [37] M. Amenomori *et al.* [Tibet ASgamma Collaboration], *Adv. Space Res.* **47**, 629 (2011).
- [38] A. P. Garyaka, R. M. Martirosov, S. V. Ter-Antonyan, A. D. Erlykin, N. M. Nikolskaya, Y. A. Gallant, L. W. Jones and J. Procureur, *J. Phys. G* **35**, 115201 (2008).
- [39] S. F. Berezhnev *et al.* [Tunka Collaboration], *Talk given at ECRS 2012*.
- [40] T. K. Gaisser, *Astropart. Phys.* **35**, 801 (2012).
- [41] J. R. Hoerandel, *Astropart. Phys.* **19**, 193 (2003).
- [42] R. Abbasi *et al.* [IceCube Collaboration], *Astrophys. J.* **718**, L194 (2010).
- [43] R. Abbasi *et al.* [IceCube Collaboration], *Astrophys. J.* **746**, 33 (2012).
- [44] A. H. Compton, I. A. Getting, *Phys. Rev.* **47** 817-821 (1935).
- [45] A. D. Erlykin and A. W. Wolfendale, *Astropart. Phys.* **25**, 183 (2006).
- [46] P. Blasi and E. Amato, *JCAP* **1201**, 011 (2012). [*arXiv* 1105.4529].
- [47] P. L. Biermann, J. K. Becker, E. S. Seo and M. Mandelartz, *arXiv* 1206.0828 (2012).
- [48] M. Santander [IceCube Collaboration], *arXiv* 1205.3969] (2012).
- [49] H. Kolanoski for the [IceCube Collaboration], To appear in *Proc. of ECRS 2012* [*arXiv* 1209.5610].
- [50] T. Stanev, T. K. Gaisser and F. Halzen, *Phys. Rev. D* **32**, 1244 (1985).
- [51] M. Ambrosio *et al.* [MACRO Collaboration], *Phys. Rev. D* **60**, 032001 (1999).
- [52] R. Abbasi *et al.* [IceCube Collaboration], *arXiv* 1208.2979 (2012).
- [53] R. Abbasi *et al.* [IceCube Collaboration], *Astrophys. J.* **689** 65-68 (2008).
- [54] P. Evenson *et al.*, *Talk given at SHINE 2012*.
- [55] T. Kuwabara *et al.* [IceCube Collaboration], in *Proc. of ICRC 2007* **1** (SH), 339-342.
- [56] T. Kuwabara and P. Evenson [IceCube Collaboration], in *Proc. of ICRC 2011* **10** (SH), 295-300.